Available online at www.sciencedirect.com
ScienceDirect
Applied Energy 85 (2008) 988–1001
APPLIED ENERGY
www.elsevier.com/locate/apenergy

Heat transfer enhancement in a tube using circular cross sectional rings separated from wall

Veysel Ozceyhan [a,*], Sibel Gunes [a], Orhan Buyukalaca [b], Necdet Altuntop [a]

[a] Department of Mechanical Engineering, Faculty of Engineering, Erciyes University, Kayseri 38039, Turkey
[b] Department of Mechanical Engineering, Faculty of Engineering and Architecture, Cukurova University, Adana 01330, Turkey

Received 31 August 2007; received in revised form 8 January 2008; accepted 18 February 2008
Available online 28 March 2008

Abstract

A numerical study was undertaken for investigating the heat transfer enhancement in a tube with the circular cross sectional rings. The rings were inserted near the tube wall. Five different spacings between the rings were considered as $p = d/2$, $p = d$, $p = 3d/2$, $p = 2d$ and $p = 3d$. Uniform heat flux was applied to the external surface of the tube and air was selected as working fluid. Numerical calculations were performed with FLUENT 6.1.22 code, in the range of Reynolds number 4475–43725. The results obtained from a smooth tube were compared with those from the studies in literature in order to validate the numerical method. Consequently, the variation of Nusselt number, friction factor and overall enhancement ratios for the tube with rings were presented and the best overall enhancement of 18% was achieved for $Re = 15{,}600$ for which the spacing between the rings is $3d$.
© 2008 Elsevier Ltd. All rights reserved.

Keywords: Heat transfer enhancement; Ring inserted tube; Pressure drop; Performance comparison

1. Introduction

Heat transfer enhancement is a subject of considerable interest to researchers as it leads to saving in energy and cost. Because of the rapid increase in energy demand in all over the world, both reducing energy lost related with ineffective use and enhancement of energy in the meaning of heat have become an increasingly significant task for design and operation engineers for many systems. In the past few decades numerous researches have been performed on heat transfer enhancement. These researches focused on finding a technique not only increasing heat transfer, but also achieving high efficiency. Achieving higher heat transfer rates through various enhancement techniques can result in substantial energy savings, more compact and less expensive equipment with higher thermal efficiency.

Heat transfer enhancement technology has been improved and widely used in heat exchanger applications; such as refrigeration, automotives, process industry, chemical industry, etc. One of the widely-used heat

* Corresponding author. Tel.: +90 352 437 4901 32108; fax: +90 352 437 5784.
E-mail address: ozceyhan@erciyes.edu.tr (V. Ozceyhan).

0306-2619/$ - see front matter © 2008 Elsevier Ltd. All rights reserved.
doi:10.1016/j.apenergy.2008.02.007

Nomenclature

a	speed of sound
d	inside diameter of the tube
G_b	turbulence kinetic energy due to buoyancy
f	friction factor
G_k	turbulence kinetic energy generation
h	convective heat transfer coeefficient
k	thermal conductivity of air
L	length of the tube
M	Mach number
Nu	Nusselt number
P	pressure
p	spacing between the rings
Pr	Prandtl number
q''	heat flux
Re	Reynolds number
r	radial coordinate
r_i	tube inner radius
r_o	tube outer radius
t	thickness of the tube
T	temperature (K)
T_{inlet}	tube inlet temperature
x	axial coordinate
U	flow velocity
r	radial coordinate
υ_x	swirl velocity
υ_r	velocity in r direction

Subscripts

ave	average
b	bulk
r	ring inserted tube
s	smooth tube
t	turbulent
w	tube wall media

Greek letters

β	the coefficient of thermal expansion
ε	turbulence kinetic energy dissipiation rate
k	Turbulent kinetic energy
μ	fluid dynamic viscosity
ρ	fluid density

transfer enhancement technique is inserting different shaped elements with different geometries in channel flow [1–5].

There exist numerous studies on heat transfer enhancement by inserting fins, twisted tapes baffles and coil wires [6–13]. The performances of shell-side heat transfer and pressure drop were experimentally studied in a helically baffled single tube heat exchanger by Zhang et al. [7]. They used one smooth tube and five petal-shaped fin tubes (PF tubes) with different geometrical parameters in order to enhance the heat transfer of

the shell side. As a result of their study, they reported that the Nusselt numbers increased with fin height and decreased with fin pitch. Tijing et al. [8] investigated the effects of star-shape fin inserts on the heat transfer and pressure drop in a concentric-tube heat exchanger. The results showed that a straight-fin configuration is the best to produce a heat transfer increase in a counterflow heat exchanger and twisted fin configurations did not further increase the heat transfer rate. Heat transfer and friction characteristics in a double pipe heat exchanger fitted with regularly spaced twisted tape elements were experimentally investigated by Eimsa-ard et al. [9]. The results showed that heat transfer coefficient increased with twist ratio whereas the increase in the free space ratio improved both the heat transfer coefficient and friction factor. Chang et al. [10] presented an original experimental study on compound heat transfer enhancement in a tube fitted with serrated twisted tape. A set of empirical correlations that permits the evaluation of the Nusselt number and the fanning friction factor in the developed flow region for the tubes fitted with smooth and serrated twisted tapes was generated for engineering applications. The effect of baffle size and orientation on the heat transfer enhancement was studied in detail by Nasiruddin [11]. The results showed that for the vertical baffle, an increase in the baffle height causes a substantial increase in the Nusselt number but the pressure loss is also very significant. For the inclined baffles, the Nusselt number enhancement is almost independent of the baffle inclination angle. The heat transfer characteristics and pressure drop results of the horizontal double tubes with coil-wire insert were presented by Naphon [12]. It was seen that the heat transfer rate and heat transfer coefficient depend directly on the mass flow rates of hot and cold water. Effect of coil-wire insert on the enhancement of heat transfer tends to decrease as Reynolds number increases.

Heat transfer enhancement by inserting ribs is commonly used application in tubes. Ribs improve the heat transfer by interrupting the wall sublayer. This yields flow turbulence, separation and reattachment leading to higher heat transfer rates. Due to the existence of ribs effective heat transfer surface increases. Many researches have been carried out on heat transfer enhancement achieved by different ribs [13–18]. San and Huang [16] performed an experimental investigation on heat transfer enhancement of transverse ribs in circular tubes. The mean Nusselt number (Nu) and friction factor (f) were individually correlated as a function of the rib pitch-to-tube diameter ratio (p/d), rib height-to-tube diameter ratio (e/d) and Re. A critical e/d, equal to 0.057, was found. For $e/d < 0.057$, the f is proportional to e/d; for $e/d \geqslant 057$, the f is proportional to $(e/d)^{2.55}$. Forced convection heat transfer of air in a rectangular channel with different angled ribs on one wall was investigated experimentally and numerically by Lu and Jiang [17]. The numerical results indicated that the heat transfer coefficients were largest with the 60° ribs, but the channel with the 20° ribs had the best overall thermal/hydraulic performance considering the heat transfer and the pressure drop when the spacing between ribs was 4 mm. Tanda [18] performed heat transfer and pressure drop experiments for a rectangular channel equipped with in-line and staggered arrays of diamond-shaped elements. Thermal performance comparisons with data for rectangular channel without diamond-shaped elements showed that the presence of the diamond-shaped elements enhanced heat transfer by a factor up to 4.4 for equal mass flow rate and by a factor up to 1.65 for equal pumping power.

The literature survey on investigations of different type of tube inserts indicates that these inserts are generally attached on the tube walls in order to enhance the heat transfer by not only disturbing the laminar sublayer and discontinuing the development of boundary layer, but also increasing the effective heat transfer area. This work differs from those in the literature by attaching the ring inserts separated from the tube wall, thus the effective heat transfer area was not increased and heat transfer enhancement was achieved by only disturbing the laminar sublayer. Furthermore it is known that attaching the inserts on the tube wall may cause contamination in time, thus there will occur an additional resistance against to heat transfer. Therefore, attaching the inserts near the wall will be convenient in the meaning of preventing the formation of contamination. In this work, the circular cross sectional rings were preferred, because in practice these rings are relatively easy to manufacture, less expensive and also relatively easy to insert and remove from the tube, thereby validating their use in heat transfer enhancement.

The present work submits a numerical study on heat transfer and friction loss characteristics of a tube with circular cross sectional ring inserts. The rings are inserted near the tube wall and the heat transfer enhancement is investigated related with the effect of spacing between the rings. Five different spacings between the rings are considered as $p = d/2$, $p = d$, $p = 3d/2$, $p = 2d$ and $p = 3d$. A uniform heat flux is applied through the external surface of the tube and the flow is assumed to be fully-developed at the inlet. The constant or

uniform heat flux boundary condition is commonly preferred in industrial applications. There are numerous works in which the constant or uniform heat flux used [19–23]. A numerical technique is used for solving the governing flow and energy equations. For the purpose of comparison and numerical method validation, calculations for a smooth tube are also performed under similar conditions.

2. Numerical modeling

A schematic view of the physical model is shown in Fig. 1a where the investigated region in this study is sketched by dotted lines and Fig. 1(b) indicates the details of investigated region. The numerical simulations were conducted in two-dimensional domain, which represents a tube of 18 mm diameter and 846 mm length. The length of the inlet section is selected long enough to provide a fully developed flow and also the length of the exit section is selected long enough to prevent the adverse pressure effects at the exit. The rings were attached near the tube wall with a clearance of 0.3 mm. Five different spacings between the rings were considered as $p = d/2$, d, $3d/2$, $2d$ and $3d$.

The computational domain, which consists of a mesh layout with approximately 815,680 cells, is presented in Fig. 2. The grid is highly concentrated near the wall and in the vicinity of the rings. For grid independence, the number of cells is varied from 532,735 to 992,556 in various steps. It is found that after 744,280 cells, further increase in cells has less than 2% variation in Nusselt number which is taken as criterion for grid independence.

The assumptions used in the mathematical model are:

- The flow is steady, fully-developed, turbulent, and two-dimensional.
- The thermal conductivity of the tube wall material does not change with temperature.
- The tube material is homogeneous and isotropic.

Numerical calculations are performed to solve the problem depending on the numerical model, boundary conditions, assumptions, and numerical values in order to determine the temperature and velocity distributions in the flow field. Segregated manner was selected as solver type. Standart k–ε turbulence model is allowed to predict the heat transfer and fluid flow characteristics by using the computational fluid dynamics (CFD) commercial code, FLUENT 6.1.22 [24]. The first order upwind numerical scheme and PISO (pressure implicit with splitting of operations) algorithm are utilized to discretize the governing equations.

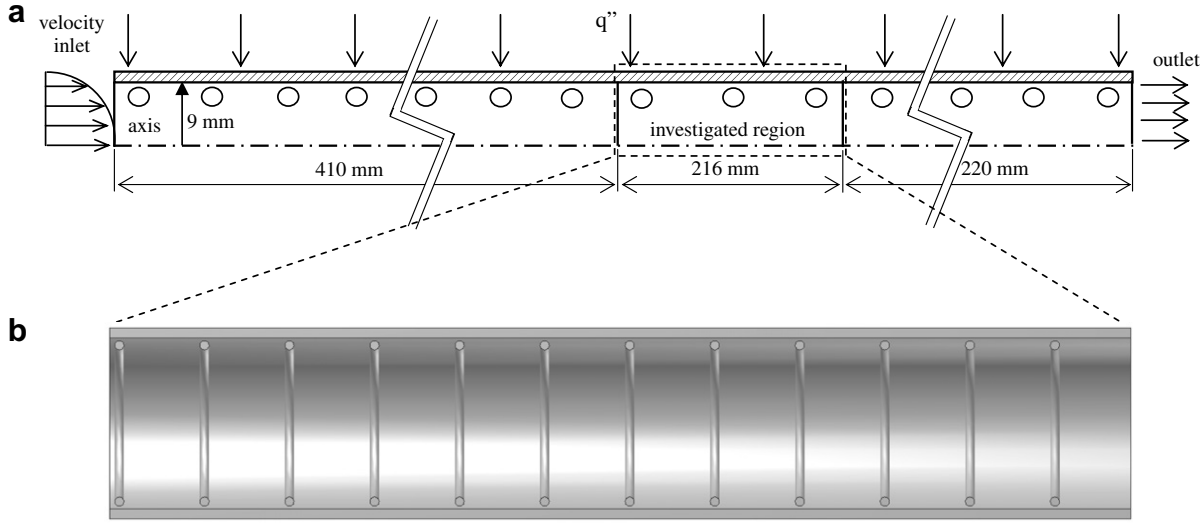


Fig. 1. (a) Physical model for ring inserted tube (b) detail of investigated region.

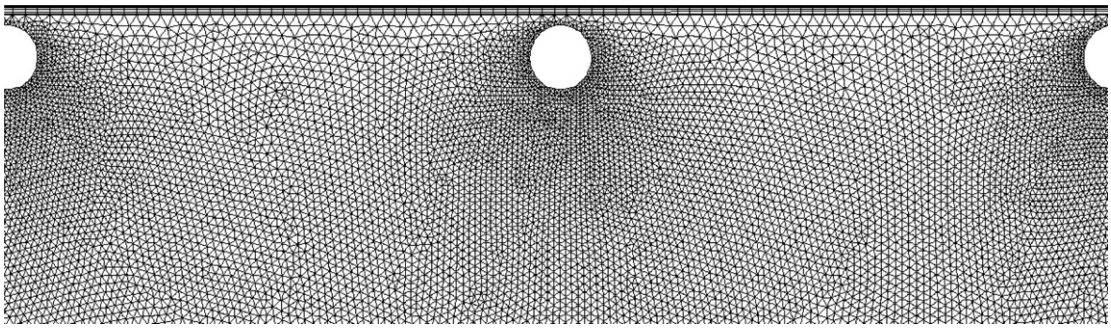


Fig. 2. Part of numerical mesh for ring inserted tube.

An eddy diffusivity approximation for the turbulent heat flux is used for the temperature field calculations. Turbulent Prandtl number (Pr_t), which has a value between 0.73 and 0.92 [25], is taken as 0.85 for all calculations as recommended by Ooi et al. [26]. The convergence criterion is selected 10^{-7} for energy and 10^{-5} for other residuals.

2.1. Governing equations

It is assumed that the problem is described by the two-dimensional, steady continuity, momentum and energy equations with constant thermophysical properties.

The continuity equation is

$$\frac{\partial}{\partial x}(\rho v_x)+\frac{\partial}{\partial r}(\rho v_r)+\frac{\rho v_r}{r}=0 \tag{1}$$

For two-dimensional axisymmetric geometries, the axial and radial momentum conservation equations are

$$\frac{1}{r}\frac{\partial}{\partial x}(r\rho v_x v_{x)}+\frac{1}{r}\frac{\partial}{\partial r}(rv_r v_x)=-\frac{\partial p}{\partial x}+\frac{1}{r}\frac{\partial}{\partial x}\left[r\mu\left(2\frac{\partial v_x}{\partial x}-\frac{2}{3}(\nabla\cdot\vec{v})\right)\right]+\frac{1}{r}\frac{\partial}{\partial r}\left[r\mu\left(\frac{\partial v_x}{\partial r}+\frac{\partial v_r}{\partial x}\right)\right]+F_x \tag{2}$$

and

$$\frac{1}{r}\frac{\partial}{\partial r}(r\rho v_x v_r)+\frac{1}{r}\frac{\partial}{\partial r}(r\rho v_r v_r)=-\frac{\partial p}{\partial r}+\frac{1}{r}\frac{\partial}{\partial x}\left[r\mu\left(\frac{\partial v_r}{\partial x}+\frac{\partial v_x}{\partial r}\right)\right]+\frac{1}{r}\frac{\partial}{\partial r}\left[r\mu\left(2\frac{\partial v_r}{\partial r}-\frac{2}{3}(\nabla\cdot\vec{v})\right)\right]-2\mu\frac{v_r}{r^2}$$
$$+\frac{2}{3}\frac{\mu}{r}(\nabla\cdot\vec{v})+\rho\frac{v_z^2}{r}+F_r \tag{3}$$

where

$$\nabla\cdot\vec{v}=\frac{\partial v_x}{\partial x}+\frac{\partial v_r}{\partial r}+\frac{v_r}{r} \tag{4}$$

In this study, Reynolds numbers are calculated from Eq. (21). The calculated range 4475–43725 is in turbulent range for a tube flow. Therefore, Standard k–ε turbulence model is used in the simulations. Despite its limitations, this model has been successfully applied to flows with engineering applications including flows in tubes. A successful application of k–ε model in predicting transport processes in a channel in presence of a triangle-shaped vortex generator was reported by Deb et al. [27]. Since the three-dimensional flow field was captured efficiently by them using the standard k–ε model, it is assumed to be convenient for the present simulation which is two-dimensional in nature. In literature, there exist various numerical studies concerning with rib inserted tube flow which are performed by using k–ε turbulence model [28–30]. In the derivation of the k–ε model, the flow is assumed to be fully turbulent and the effects of molecular viscosity are negligible. The turbulence kinetic energy, k, and its rate of dissipation, ε, are obtained from the following transport equations [24,31]:

$$\frac{\partial}{\partial x}(\rho k v_x) = \frac{\partial}{\partial r}\left[\left(\mu + \frac{\mu_t}{\sigma_k}\right)\frac{\partial k}{\partial r}\right] + G_k + G_b - \rho\varepsilon - Y_M \tag{5}$$

$$\frac{\partial}{\partial x}(\rho \varepsilon v_x) = \frac{\partial}{\partial r}\left[(\mu + \frac{\mu_t}{\sigma_\varepsilon})\frac{\partial \varepsilon}{\partial r}\right] + C_{1\varepsilon}\frac{\varepsilon}{k}(G_k + C_{3\varepsilon}G_b) - C_{2\varepsilon}\rho\frac{\varepsilon^2}{k} \tag{6}$$

In these equations, G_k represents the generation of turbulence kinetic energy due to the mean velocity gradients and it is expressed as

$$G_k = -\rho v_x' v_r' \frac{\partial v_r}{\partial x} \tag{7}$$

and G_b is the generation of turbulence kinetic energy due to buoyancy and expressed as

$$G_b = \beta g_x \frac{\mu_t}{Pr_t}\frac{\partial T}{\partial x} \tag{8}$$

The coefficient of thermal expansion is defined as

$$\beta = -\frac{1}{\rho}\left(\frac{\partial \rho}{\partial T}\right)_P \tag{9}$$

The term Y_M in Eq. (5) represents the contribution of the fluctuating dilatation in compressible turbulence to the overall dissipation rate and it is included in the k equation. This term is modeled based on the proposal by Sarkar and Balakrishnan [32] as

$$Y_M = 2\rho\varepsilon M_t^2 \tag{10}$$

where M_t is the turbulent Mach number

$$M_t = \sqrt{\frac{k}{a^2}} \tag{11}$$

and

$$a \equiv \sqrt{\gamma RT} \tag{12}$$

is the speed of the sound. $C_{1\varepsilon}$, $C_{2\varepsilon}$, and $C_{3\varepsilon}$ are constants and σ_k and σ_ε are the turbulent Prandtl numbers for k and ε, respectively. The turbulent (or eddy) viscosity may be determined from:

$$\mu_t = \rho C_\mu \frac{k^2}{\varepsilon} \tag{13}$$

where C_μ is a constant. The model constants $C_{1\varepsilon}$, $C_{2\varepsilon}$, $C_{3\varepsilon}$, σ_k, and σ_ε have the following values [33]:

$$C_{1\varepsilon} = 1.44, \quad C_{2\varepsilon} = 1.92, \quad C_{3\varepsilon} = 0.09, \quad C_\mu = 1, \sigma_k = 1.0, \quad \sigma_\varepsilon = 1.3.$$

These default values were determined from experiments with air and water for fundamental turbulent shear flows including homogeneous shear flows and decaying isotropic grid turbulence [24].

In the solid side, the two-dimensional governing conduction equation is

$$\frac{1}{r}\frac{\partial}{\partial r}\left(r\frac{\partial T}{\partial r}\right) + \frac{\partial^2 T}{\partial x^2} = 0 \tag{14}$$

2.2. Boundary conditions

The solution domain of the considered $2d$, axisymmetric tube flow is geometrically quite simple, which is a rectangle on the x–r plane, enclosed by the inlet, outlet, axis and wall boundaries. On walls, no-slip conditions ($r = R$, $v_z = v_r = 0$) are used for the momentum equations. In order to determine the value of heat flux, the simulations were conducted for heat flux of 1500, 2500, 3500 and 5000 W/m^2. It is seen that heat flux has less than 2% variation in Nusselt number and friction factor. Therefore the wall boundary condition is selected as

Table 1
The thermophysical data of the air at 300 K

T (K)	ρ (kg/m^3)	c_p (kJ/kg K)	$\mu \times 10^7$ (Ns/m^2)	$v \times 10^6$ (m^2/s)	$k \times 10^3$ (W/m K)	$\alpha \times 10^6$ (m^2/s)
300	1.1614	1.007	184.6	15.89	26.3	22.5

constant heat flux of 2500 W/m^2. At the tube inlet, parabolic velocity profile [$U_r = 2 \times U_m(1\text{-}(r/R)^2)$] is prescribed in order to keep the hydrodynamic entrance length to be short and the temperature of working fluid is set equal to 300 K at the inlet of tube. The temperature of air inside the tube is also taken as 300 K at the beginning. The thermophysical data of the air at 300 K is given in Table 1. The outlet boundary condition is natural condition ($\partial v_x/\partial x = \partial v_r/\partial r = 0$), which implies zero-gradient conditions at the outlet.

3. Calculation of heat transfer and friction factor

The Nusselt number is calculated as follows:

$$\mathrm{Nu} = \frac{hd}{k_\mathrm{b}} \tag{15}$$

in which k_b and h are the bulk thermal conductivity and the average heat transfer coefficient of fluid, respectively:

$$k_\mathrm{b} = 0.02418\left(\frac{T_\mathrm{b}}{273}\right)^{0.85} \tag{16}$$

for $T_\mathrm{b} = 233$–413 K

$$h = \frac{1}{L}\int_0^L h(x)\,\mathrm{d}x \tag{17}$$

where local heat transfer coefficient $h(x)$ is defined as

$$h(x) = \frac{q''}{T_w(x) - T_\mathrm{b}(x)} \tag{18}$$

q'' represents the heat flux. $T_\mathrm{w}(x)$ and $T_\mathrm{b}(x)$ are the local wall and bulk temperatures, respectively. $T_\mathrm{b}(x)$ can be found from:

$$T_\mathrm{b}(x) = \frac{1}{U_\mathrm{m}A}\int_0^r T_\mathrm{b}(r)\cdot U(r)\cdot \mathrm{d}A \tag{19}$$

in which U_m is mean velocity:

$$U_\mathrm{m} = \frac{1}{A}\int_0^r U(r)\cdot \mathrm{d}A \tag{20}$$

The Reynolds number and friction factor are defined by:

$$Re = \frac{\rho U_\mathrm{m} D}{\mu} \tag{21}$$

where ρ and μ are density and dynamic-viscosity of fluid, respectively.

$$\rho = 348.1\frac{p}{T_\mathrm{b}} \tag{22}$$

for $p = 1$ atm and $T_\mathrm{b} = 173$–373 K.

$$\mu = 1.724.10^{-5}\left(\frac{T_\mathrm{b}}{273}\right) \tag{23}$$

for $T_\mathrm{b} = 253$–433 K.

The friction factor is calculated as follows;

$$f = \frac{\Delta P}{\frac{1}{2}\rho \cdot U_{\mathrm{m}}^2 \frac{L}{d}} \tag{24}$$

in which pressure ΔP is pressure difference between inlet and exit:

$$\Delta P = P_{\mathrm{ave,inlet}} - P_{\mathrm{ave,outlet}} \tag{25}$$

Here, $P_{\mathrm{ave,inlet}}$ and $P_{\mathrm{ave,outlet}}$ are the inlet and outlet average pressures, respectively. Average pressure P_{ave} can be calculated from:

$$P_{\mathrm{ave}} = \frac{1}{A}\int_0^r P(r) \cdot \mathrm{d}A \tag{26}$$

4. Results and discussion

First of all, Nusselt number and friction factor are obtained for a smooth tube to validate the numerical procedure developed. The results of Nusselt number and friction factor for smooth tube are compared with the results obtained from the well-known steady state flow correlations of Petukhov [34], Gnielinski [35] and Moddy [36] for the fully developed turbulent flow in circular tubes.

Nusselt number correlation from Petukhov [34] is of the following form for $10^4 \leqslant \mathrm{Re} \leqslant 5 \times 10^6$:

$$Nu = \frac{\left(\frac{f}{8}\right) RePr}{1.07 + 12.7\left(\frac{f}{8}\right)^{\frac{1}{2}}\left(Pr^{\frac{2}{3}} - 1\right)} \tag{27}$$

Gnielinski [35] correlation as given in Eq. (24) is used to find out heat transfer in smooth tube:

$$Nu = \frac{\lambda}{8}\left(\frac{(Re - 100)Pr}{1 + 12.7\left(\frac{\lambda}{8}\right)^{\frac{1}{2}}\left(Pr^{\frac{2}{3}} - 1\right)}\right) \tag{28}$$

where

$$\lambda = \frac{1}{1.82(\log(Re) - 1.64)^2} \tag{29}$$

Gnielinski equation is valid for $2300 \leqslant Re \leqslant 5 \times 10^4$.

The friction factor correlation from Moody [36] is of the form:

$$f = 0.316Re^{-\frac{1}{4}} \quad \text{for } Re \leqslant 20000 \tag{30}$$

$$f = 0.184Re^{-\frac{1}{5}} \quad \text{for } Re \geqslant 20000 \tag{31}$$

Correlation from Petukhov [34] is of the form:

$$f = (0.79\mathrm{In}Re - 1.64)^{-2} \quad \text{for } 3000 \leqslant Re \leqslant 5 \times 10^6 \tag{32}$$

Figs. 3 and 4 show comparison between the results of the present numerical study and the well-known correlations for steady state flow conditions for smooth tube. As seen in these figures, there is a good agreement between the results for the present smooth tube and correlations in the literature. These results give confidence that the numerical method used was accurate.

In this work, the used numerical method to obtain results is also validated using experimental results. For this purpose, we use the work of Eimsa-ard and Promvonge [1], in which a circular tube fitted with V-nozzle turbulators for different pitch ratios. The correlation of Nusselt number and friction factor for a circular tube fitted with V-nozzle turbulators are given by;

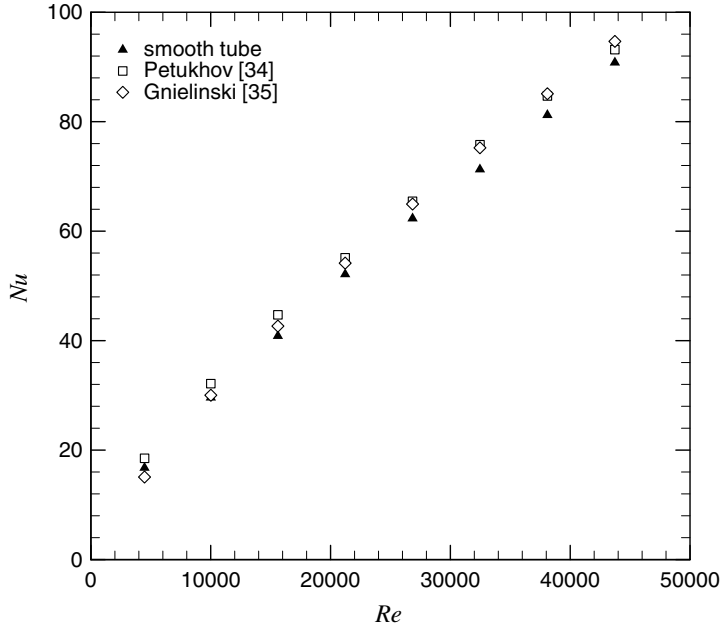


Fig. 3. Data verification of Nusselt number for smooth tube.

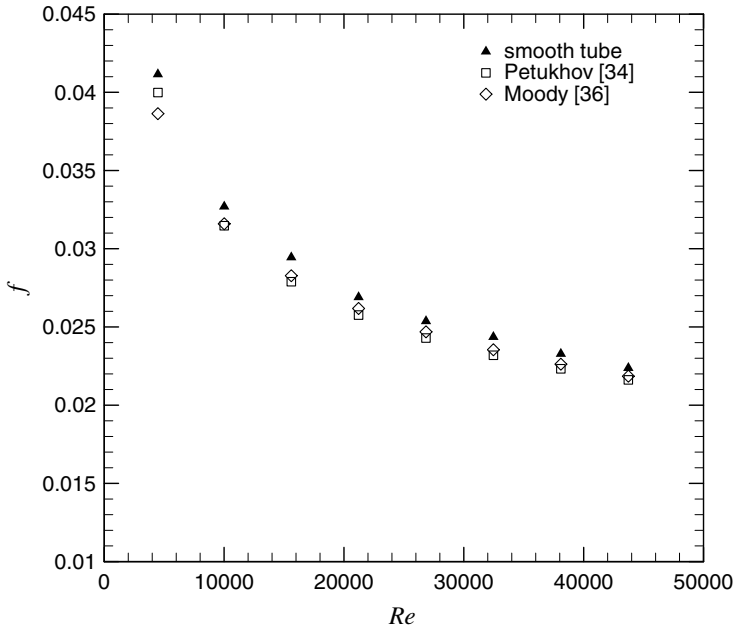


Fig. 4. Data verification of friction factor for smooth tube.

$$Nu = 0.524 Re^{0.6} Pr^{0.4} (PR)^{-0.285} \tag{33}$$

$$f = 107 Re^{-0.42} (PR)^{-0.68} \tag{34}$$

where PR is pitch ratio. The simulations are conducted for the value of PR is 4.

The comparison of results by our numerical method and experimental results of Eimsa-ard and Promvonge [1] shows very good agreement as illustrated in Figs. 5 and 6. The results of our numerical method agree

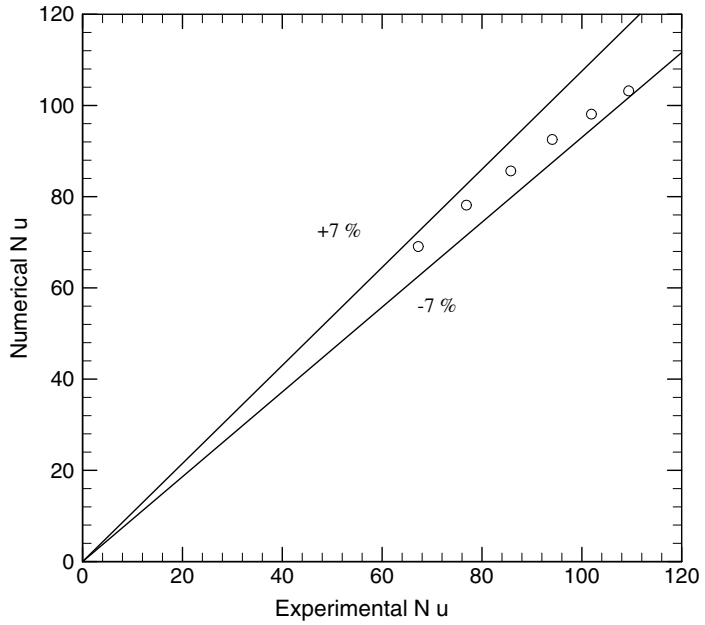


Fig. 5. Comparison of numerical and experimental values of Nusselt number.

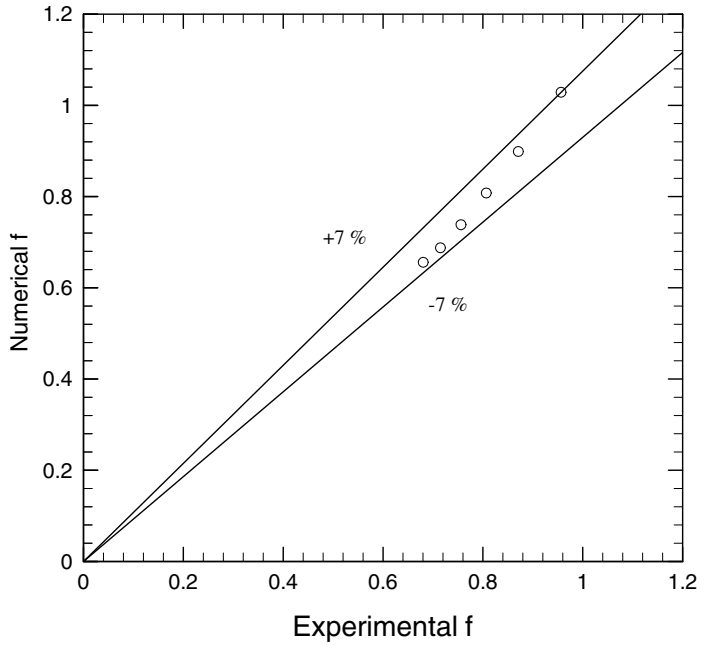


Fig. 6. Comparison of numerical and experimental values of friction factor.

reasonably well with the fitted correlations within ±7% in comparison with experimental data for Nusselt number and friction factor.

This article presents the numerical results of both heat transfer and pressure drop in circular cross sectioned ring inserted tube for steady state condition. The variation of Nusselt number with Reynolds number for all cases is plotted in Fig. 7. It is clear from this figure that Nusselt number increases with the increase of Reynolds number, as expected.

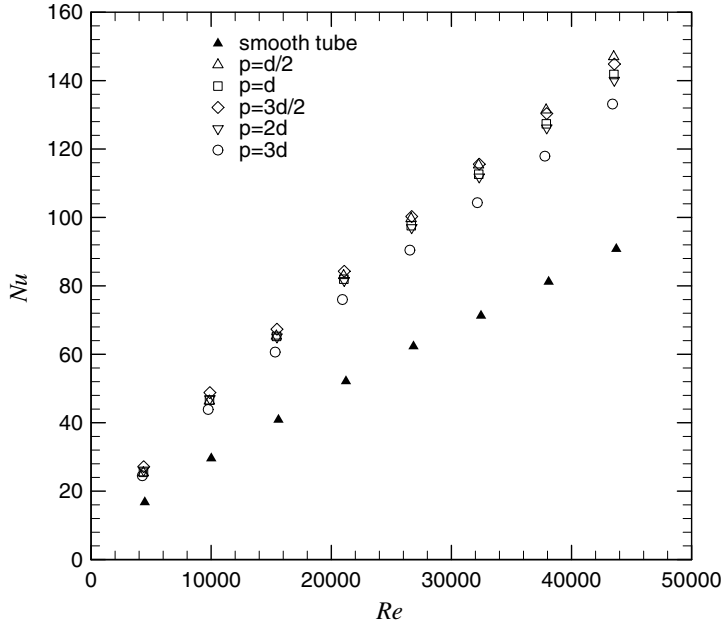


Fig. 7. Variation of Nusselt number with Reynolds number for different ring spacings.

It is observed from Fig. 7 that the tubes with rings introduce higher heat transfer rate than the smooth tube. Decrease in the distance between the rings (p) leads to a higher Nusselt number. Therefore, the highest Nusselt number is achieved in the case of $p = d/2$.

As mentioned earlier, the rings are attached near the wall with a clearance of 0.3 mm. Thus, the clearance between the wall and the rings cause higher velocities occur in the clearance gap, and consequently heat transfer increases. Flow passes through the clearance between the wall and rings and heat transfer results with an increase because of the flow disturbance near the wall region due to the rings.

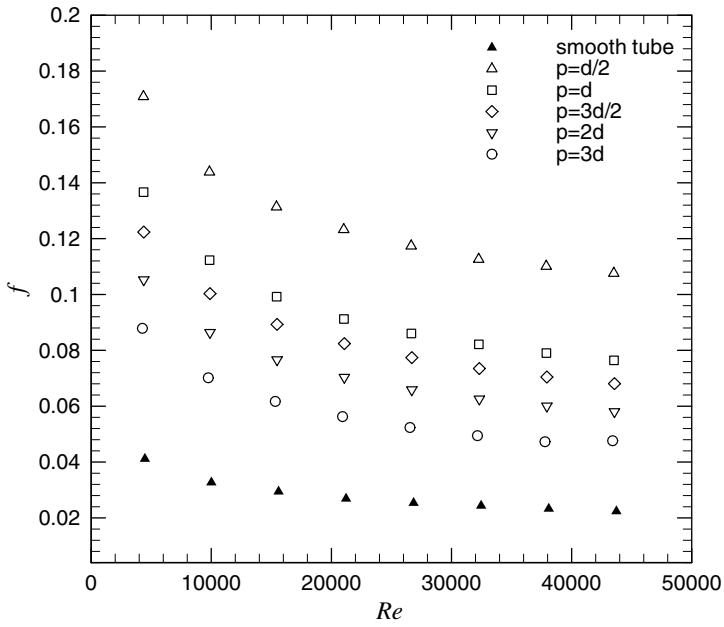


Fig. 8. Variation of friction factor with Reynolds number for different ring spacings.

On the other hand, as expected, these inner ribs cause a significant pressure drop as well, in comparison with the smooth tube. The increase in Nusselt number results in an increase in pressure drop, the friction factor increases with decreasing ring spacings due to the fact that increasing the number of rings disturb the entire flow field and cause more friction. The friction factor decreases with increasing Reynolds numbers, as indicated in Fig. 8. The slope of friction factor curves decreases for high Reynolds numbers and the highest friction factor is obtained when the spacing between the rings is $d/2$ in which there is more flow resistance.

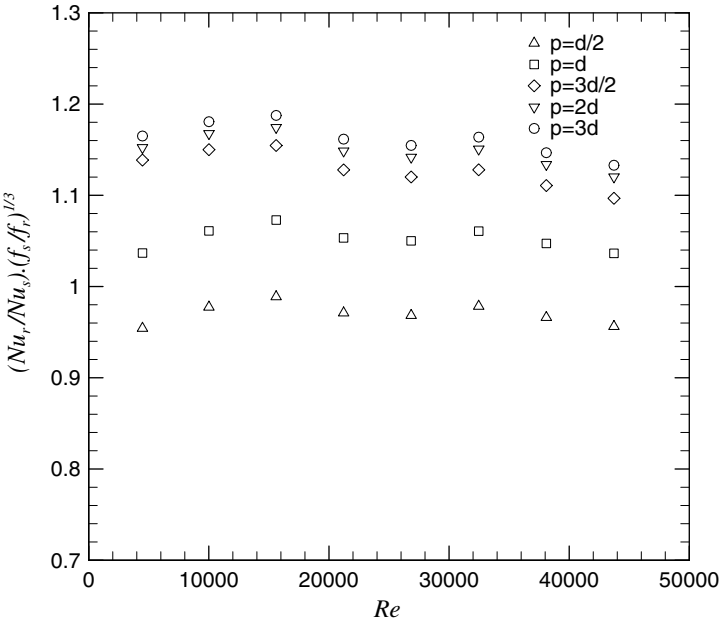


Fig. 9. Overall enhancement ratio for different ring spacings.

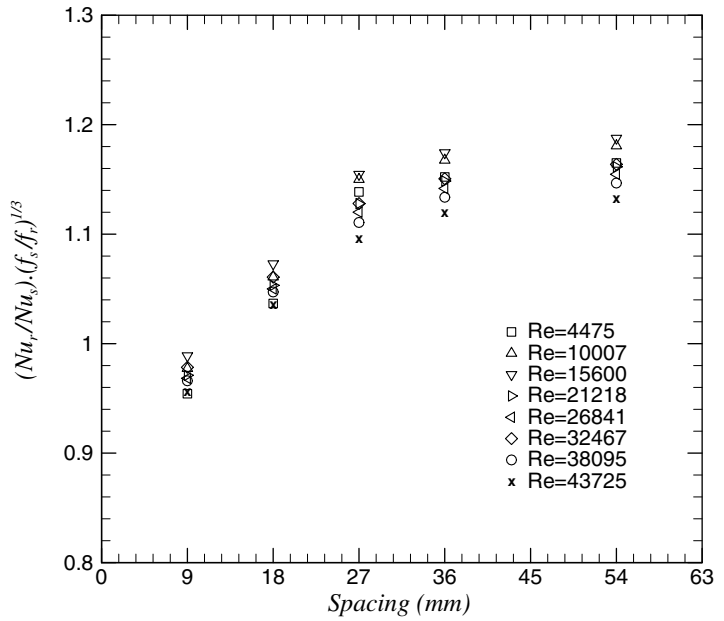


Fig. 10. Overall enhancement ratio versus ring spacings.

Heat transfer enhancement is obtained at the expense of increased pressure drop caused by tube insertions. Therefore, a performance analysis is important for the evaluation of the net energy gain to determine if the method employed to increase the heat transfer is effective from energy point of view. In order to determine the net final gain, the parameter $(Nu_r/Nu_s) \cdot (f_s/f_r)^{1/3}$ is used [37] as the overall enhancement ratio, which means the comparison is made based on constant pumping power. Fig. 9 illustrates the overall enhancement ratio for all cases. It is seen from Fig. 9 that the overall enhancement ratio increases with the increase in ring spacings.

There will be a net energy gain only $(Nu_r/Nu_s) \cdot (f_s/f_r)^{1/3}$ is greater than unity. So, it is evident from Fig. 9 that for all cases except the case of $p = d/2$, the overall enhancement ratio is greater than unity. Due to the increase in friction factor is more effective than the increase in heat transfer for the case of $p = d/2$, the overall enhancement ratio is the worst contrary to Nusselt numbers values. This spacing is not efficient in terms of overall performance because the fluid friction dominates the heat transfer, so the use of these rings with a spacing of $d/2$ is not thermodynamically advantageous. The best overall enhancement of 18% was achieved for $Re = 15{,}600$ in which the spacing between the rings is $3d$.

Fig. 10 shows the overall enhancement ratios versus ring spacings. It is observed from this figure that the overall enhancement ratios increase with the increase in ring spacings. The overall enhancement ratios for $p = 2d$ and $p = 3d$ are almost the same and this means that the overall enhancement ratio does not change considerably after the case of $p = 2d$. Consequently, it may be expected that the overall enhancement ratios tend to decrease, for the ring spacings greater than $3d$.

5. Conclusions

The fundamental objective of this study is to investigate the heat transfer and pressure drop in circular cross sectioned rings inserted tube. A numerical study is performed to determine the effect of attaching the rings near the wall and the ring spacing on the heat transfer and friction characteristics within the range of Reynolds number from 4475 to 43725. In this study constant pumping power criterion is used to evaluate the overall performance of five different cases ($p = d/2$, d, $3d/2$, $2d$ and $3d$). The following conclusions can be derived as:

- For all cases, Nusselt number increases and friction factor decreases with increasing Reynolds number. The highest Nusselt number and friction factor is obtained in the case of $p = d/2$.
- The Nusselt number and friction factor increase with decreasing ring spacing. As expected $p = d/2$ type insert introduces more pressure drop than the other types.
- Except the case of $p = d/2$, the overall enhancement ratios are higher than unity for all investigated cases. The fluid friction dominates the heat transfer, so the use of these rings with a spacing of $d/2$ is not thermodynamically advantageous on the basis of heat transfer enhancement.
- The overall enhancement ratio increases with increasing ring spacing. Therefore, the best overall enhancement of 18% was achieved for $Re = 15{,}600$ in which the spacing between the rings is $3d$. The spacing of $p = d$, $3d/2$ and $2d$ are also efficient in terms of overall performance.

Acknowledgements

Authors would like to thank for the financial support of the Scientific Research Project Division of Erciyes University under the contract: FBT-07-54.

References

[1] Eimsa-ard S, Promvonge P. Experimental investigation of heat transfer and friction characteristics in a circular tube fitted with V-nozzle turbulators. Int Commun Heat Mass Transfer 2006;33:591–600.
[2] Khaled RA. Heat transfer enhancement in hairy fin systems. Appl Therm Eng 2007;27:250–7.
[3] Shoji Y, Sato K, Oliver DR. Heat transfer enhancement in round tube using wire coil influence of length and segmentation. Heat Transfer-Asian Res 2003;32(2):99–107.
[4] Zimparov V. Enhancement of heat transfer by a combination of three-start spirally corrugated tubes with a twisted tape. Int J Heat Mass Transfer 2001;44:551–74.

[5] Tandiroglu A, Ayhan T. Energy dissipation analysis of transient heat transfer for turbulent flow in a circular tube with baffle inserts. Appl Therm Eng 2006;26:178–85.
[6] Yakut K, Alemdaroglu N, Sahin B, Celik C. Optimum design-parameters of a heat exchanger having hexagonal fins. Appl Energy 2006;83:82–98.
[7] Zhang Z, Yu Z, Fang X. An experimental heat transfer study for helically flowing outside petal-shaped finned tubes with different geometrical parameters. Appl Therm Eng 2007;27:268–72.
[8] Tijing LD, Pak BC, Baek BJ, Lee DH. A study on heat transfer enhancement using straight and twisted internal fins. Int Commun Heat Mass Transfer 2006;33:719–26.
[9] Eimsa-ard S, Thianpong C, Promvonge P. Experimental investigation of heat transfer and flow friction in a circular tube fitted with regularly spaced twisted tape elements. Int Commun Heat Mass Transfer 2006;33:1225–33.
[10] Chang SW, Jan YJ, Liou JS. Turbulent heat transfer and pressure drop in tube fitted with serrated twisted tape. Int J Therm Sci 2007;46:506–18.
[11] Shaikh N, Siddiqui MHK. Heat transfer augmentation in a heat exchanger tube using a baffle. Int J Heat Fluid Flow 2007;28:318–28.
[12] Naphon P. Effect of coil-wire insert on heat transfer enhancement and pressure drop of horizontal concentric tubes. Int Commun Heat Mass Transfer 2006;33:753–63.
[13] Buchlin JM. Convective heat transfer in a channel with perforated ribs. Int J Therm Sci 2002;41:332–40.
[14] Tanda G. Heat transfer in rectangular channels with transverse and V-shaped broken ribs. Int J Heat Mass Transfer 2004;47:229–43.
[15] Jordan SA. The turbulent character and pressure loss produced by symmetric ribs in a circular duct. Int J Heat Fluid Flow 2003;24:795–806.
[16] San JY, Huang WC. Heat transfer enhancement of transverse ribs in circular tubes with consideration of entrance effect. Int J Heat Mass Transfer 2006;49:2965–71.
[17] Lu B, Jiang PX. Experimental and numerical investigation of convection heat transfer in a rectangular channel with angled ribs. Exp Therm Fluid Sci 2006;30:513–21.
[18] Tanda G. Heat transfer and pressure drop in a rectangular channel with diamond-shaped elements. Int J Heat Mass Transfer 2001;49:3529–41.
[19] Promvonge P, Eimsa-ard S. Heat transfer augmentation in a circular tube using V-nozzle turbulator inserts and snail entry. Exp Therm Fluid Sci 2007;32:332–40.
[20] Promvonge P, Eimsa-ard S. Heat transfer in a circular tube fitted with free-spacing snail entry and conical-nozzle turbulators. Int Commun Heat Mass Transfer 2007;34:838–48.
[21] Sahin B, Demir A. Performance analysis of a heat exchanger having perforated square fins. Appl Therm Eng 2008;28:621–32.
[22] Gül H, Evin D. Heat transfer enhancement in a circular tubes using helical swirl generator insert at the entrance. Int J Therm Sci 2007;46:1297–303.
[23] Akansu SO. Heat transfers and pressure drops for porous-ring turbulators in a circular pipe. Appl Energy 2006;83:280–98.
[24] FLUENT 6.1.22. User's Guide. Fluent Incorporated. Centerra Resource Park, 10 Cavendish Court, Lebanon, NH 03766, USA; 2001.
[25] Kays WM. Turbulent Prandtl number – where are we? J Heat Transfer 1994;116(2):284–95.
[26] Ooi A, Iaccarino G, Durbin PA, Behnia M. Reynolds averaged simulation of flow and heat transfer in ribbed ducts. Int J Heat Fluid Flow 2002;23:750–7.
[27] Deb P, Biswas G, Mitra NK. Heat transfer and flow structure in laminar and turbulent flows in a rectangular channel with longitudinal vortices. Int J Heat Mass Transfer 1995;38:2427–44.
[28] Hiseh SS, Chang LC, Yang TY. Developing 3-D turbulent mixed convection in a circular duct inserted with longitudinal strips. Int J Eng Sci 2001;39:1327–50.
[29] Hung CI, Lin YS, Chen JD. Numerical study of heat transfer enhancement of a horizontal tube with an eccentrically inserted plate. Int J Heat Mass Transfer 1997;40:1687–92.
[30] Mon MS, Gross U. Numerical study of fin-spacing effects in annular finned tube heat exchangers. Int J Heat Mass Transfer 2004;47:1953–64.
[31] Davidson L. An introduction to turbulence models. Sweden: Göteburg; 2003.
[32] Sarkar S, Balakrishnan L. Application of a Reynolds-Stress turbulence model to the compressible shear layer. ICASE Report 1990; 90-18. NASA CR 182002.
[33] Launder BE, Spalding DB. Lectures in mathematical models of turbulence. London, England: Academic Press; 1972.
[34] Petukhov BS. Heat transfer in turbulent pipe flow with variable physical properties. In: Harnett JP, editor. Advances in heat transfer, vol. 6. New York: Academic Press; 1970. p. 504–64.
[35] Gnielinski V. New equations for heat and mass transfer in turbulent pipe flow and channel flow. Int Chem Eng 1976;16:359–68.
[36] Moody LF. Friction factors for pipe flow. Trans ASME 1944;66:671–84.
[37] Wang L, Sunden B. Performance comparison of some tube inserts. Int Commun Heat Mass Transfer 2002;29:45–56.